S-Adenosylmethionine Depletion Activates La Ribonucleoprotein Domain Family Member 1 to Induce Protein Translation

Komal Ramani[1]*, Aaron E. Robinson[2,4]*, Joshua Berlind[3]*, Wei Fan[1], Aushinie Abeynayake[1], Aleksandra Binek[4], Lucía Barbier-Torres[1], Mazen Noureddin[1,5], Nicholas N. Nissen[5,6], José M. Mato[7], Jennifer Van Eyk[4]†, Shelly C. Lu[1]†

[1]Division of Digestive and Liver Diseases, Department of Medicine, Cedars-Sinai Medical Center, Los Angeles, CA 90048; [2]Department of Genetics, Stanford University School of Medicine, Stanford, CA 94305; [3]Stem Cell Biology and Regenerative Medicine, University of Southern California, Los Angeles, CA 90033; [4]Smidt Heart Institute and Advanced Clinical Biosystems Research Institute, [5]Comprehensive Transplant Center, [6]Department of Surgery, Cedars-Sinai Medical Center, Los Angeles, CA 90048; [7]CIC bioGUNE, Centro de Investigación Biomédica en Red de Enfermedades Hepáticas y Digestivas (Ciberehd), Technology, Derio, Bizkaia 48160, Spain

*Share equal authorship

†Co-corresponding authors

To whom correspondence to be addressed:

Shelly C. Lu, M.D., Director, Division of Digestive and Liver Diseases, Department of Medicine, Cedars-Sinai Medical Center, Davis Building, Room #2097, 8700 Beverly Blvd., Los Angeles, CA, 90048. Tel: (310) 423-5692, Fax: (310) 423-0653, Email: shelly.lu@cshs.org.

COMPETING INTERESTS STATEMENT: The authors declare no competing interests.

ABSTRACT

S-adenosylmethionine (SAMe) is the principal methyl donor synthesized by methionine adenosyltransferase 1A (*MAT1A*)-encoded enzyme in the liver. Mice lacking *Mat1a* have hepatic SAMe depletion, spontaneous development of non-alcoholic steatohepatitis (NASH) and hepatocellular carcinoma (HCC). To understand how SAMe depletion drives liver pathologies we performed phospho-proteomics in *Mat1a* knockout (KO) mice livers and the most striking change was hyperphosphorylation of La-Related Protein 1 (LARP1), which in the unphosphorylated form negatively regulates translation of 5'-terminal oligopyrimidine (TOP)-containing mRNAs. Consistently, multiple TOP proteins are induced in the KO livers. We identified LARP1-T449 as a novel, SAMe-sensitive phospho-site of cyclin-dependent kinase 2. LARP1-T449 phosphorylation induced global translation, cell growth, migration, invasion, and expression of oncogenic TOP-ribosomal proteins in HCC cells. LARP1 expression is increased in human NASH and HCC. Our results reveal a novel SAMe-sensitive mechanism of LARP1 phosphorylation that may be involved in the progression of NASH to HCC.

INTRODUCTION

The methionine adenosyltransferase 1A (*MAT1A*)-encoded enzyme, MATα1, uses methionine as a substrate for the synthesis of the biological methyl donor, S-adenosylmethionine (SAMe) in the liver[1]. *MAT1A* is downregulated in non-alcoholic fatty liver disease (NAFLD) with advanced fibrosis, emphasizing an important role of SAMe metabolism in NAFLD pathogenesis in humans[2]. Patients with NAFLD with or without cirrhosis are at higher risk for hepatocellular carcinoma (HCC) development[3]. Such patients have impaired methionine metabolism as demonstrated by hypermethioninemia and reduced levels of SAMe[3].

Mice lacking *Mat1a* have chronic hepatic SAMe deficiency, spontaneous development of non-alcoholic steatohepatitis (NASH) at 8 months of age and HCC by 18 months[1,4]. Replenishment of SAMe reserves in the *Mat1a*-knockout (KO) not only prevents NASH progression, it also inhibits the development of proliferative nodules[5]. Importantly nearly 50% of NAFLD patients have a similar serum metabolomics signature as *Mat1a*-KO mice[5]. We previously observed *Mat1a*-KO livers have activation of multiple kinases, some of which may be involved in the liver pathology observed[1]. However, how deficiency of the methyl donor impacts on the phospho-proteome has not been examined.

La Ribonucleoprotein Domain Family Member 1 (also known as La-Related Protein 1, LARP1) belongs to a family of La-motif containing proteins that regulate the translation of a class of mRNAs containing a 5'-terminal oligopyrimidine tract (TOP) such as those encoding ribosomal proteins (RPs) and translation initiation/elongation factors[6]. LARP1 inhibits translation of TOP mRNAs by simultaneously binding to their 5'-TOP and 3'-UTR elements[7,8]. Recently LARP1 has been identified as the missing link between mammalian target of rapamycin C1 (mTORC1) and ribosome biogenesis. Phosphorylation of LARP1 by mTORC1 (at S689 and T692) and AKT/S6K1

(at S770 and S979) induces its dissociation from the oligopyrimidine tract relieving its inhibitory activity on RP mRNA translation[7,9]. Phosphorylated LARP1 enhances mTORC1 occupancy on the 3'-UTR of RP mRNAs to facilitate mTORC1-dependent translation initiation[9]. LARP1 stabilizes TOP mRNAs because its silencing is known to induce TOP mRNA decay[6,10]. In essence, LARP1 acts as a control point for RP mRNA translation. The switch of LARP1 between phosphorylated and unphosphorylated states regulates RP mRNA translation and subsequent ribosome biogenesis[7].

During ribosomal biogenesis, RPs are synthesized in the cytoplasm and assembled with ribosomal RNA in the nucleolus[11]. Free RPs not used for ribosome assembly are rapidly turned over. However, stimuli such as nutrient deprivation, gene mutations and chemical agents may cause ribosomal stress leading to accumulation of free RPs[11]. Accumulating evidence suggests that free RPs exhibit extra-ribosomal functions associated with oncogenesis or tumor suppression[12], and their dysregulation has been reported in NAFLD and HCC[13,14]. LARP1 as well as many oncogenic RPs are induced in HCC[12,14,15]. HCC patients with high LARP1 expression have lower survival[16].

In this work we identified LARP1 protein is hyperphosphorylated at specific sites in *Mat1a*-KO livers and SAMe-deficient cell line derived from *Mat1a*-KO HCC (SAMe-D). These SAMe deficiency models exhibit enhanced LARP1 content and TOP mRNA-encoded protein expression. SAMe treatment in these models inhibits LARP1 expression, LARP1 phosphorylation, and TOP-protein expression. Importantly, LARP1 content and several TOP-proteins are upregulated in human NASH and HCC. Taken together, our results suggest activation of LARP1 during SAMe deficiency may cause dysregulation of oncogenic TOP protein translation favoring progression of NASH to HCC.

RESULTS

Phosphoproteomics show SAMe deficiency results in an increase in protein translation machinery and hyperphosphorylation of LARP1

Using phospho-peptides enriched via TiO2 affinity chromatography, we identified specific serine/threonine phospho-sites affected in 4-month or 10-month old WT, 4-month or 10-month *Mat1a*-KO treated with SAMe or vehicle. Phosphorylation of unique peptides was normalized to that of total protein and the fold change of KO versus WT or KO+SAMe versus KO was calculated. Out of a repertoire of 4,172 phospho-peptides quantified, 355 phospho-peptides exhibited an induction in *Mat1a* KO compared to WT, which was reversed upon SAMe administration. Skyline documents containing extracted XIC from phospho-peptide enrichment experiments are available at Panorama (proteome exchange ID: PXD020015, https://panoramaweb.org/Larp1). We found that LARP1 phospho-sites were significantly represented in this repertoire. These phosphorylation sites were conserved between mouse and human (Table 1). Out of nine LARP1 sites identified, four (T449, S471, S697, S250) exhibited significant enhancement of phosphorylation in 4-month (pre-disease condition) and 10-month (NASH condition) compared to their respective WT controls (Table 1). Moreover, the phosphorylation of these sites was strongly inhibited by SAMe administration (Table 1). Since many physiologically relevant phosphorylation sites in vivo may not be abundant enough to accurately detect by mass spectrometry, we mapped SAMe-sensitive LARP1 phosphorylation sites in SAMe-D cells overexpressing *LARP1* (Table 2). The T449, S471, and S697 sites were inhibited by 40-70% upon SAMe treatment; however, in this system the S250 site was not significantly inhibited by SAMe (Table 2). Other novel sites, S843 and S444 that were not accurately detectable in the *Mat1a*-KO system (Table 1), were found to be significantly inhibited by SAMe in LARP1-overexpressing SAMe-D cells (Table 2). The T101-LARP1 site that exhibited strong induction (9-fold versus WT) in 10-month KO and was inhibited by SAMe (Table 1), could not be detected in the LARP1-overexpressing SAMe-D cells (Table 2).

Out of the nine sites, seven are novel sites not reported previously. Using multiple prediction algorithms[17,18], four of these novel sites were predicted to be phosphorylated by cyclin-dependent kinase 2 (CDK2), two by casein kinase 2 (CK2) and one site could not be assigned to a kinase. A previously published mTOR site (S689)[7] was neither responsive to SAMe deficiency nor inhibited by SAMe treatment (Tables 1 and 2). Consistent with LARP1 hyperphosphorylation, we found an enrichment in the total proteome of translational factors (RPs and translation initiation/elongation) whose expression was normalized by SAMe treatment (https://panoramaweb.org/Larp1), some of these are known to be regulated by LARP1[6].

LARP1 protein expression is increased during SAMe deficiency and reduced by SAMe treatment

Total LARP1 protein levels and mTOR activity (pSer-2448 phosphorylation) were higher in *Mat1a*-KO livers compared to WT and were inhibited by SAMe administration (Figure 1A). SAMe deficiency did not influence *Larp1* mRNA levels (Figure 1A). PhosTag™ analysis confirmed the phosphoproteomics data showing that LARP1 phosphorylation (indicated by phospho-shift or retarded band) was increased in *Mat1a*-KO livers and inhibited by SAMe administration (Figure 1B). Removal of LARP1's phosphate groups by alkaline phosphatase treatment prevented its binding to phosTag™ and caused loss of phospho-shift (Figure 1B). Low SAMe level raised LARP1 expression (Figure 1A) as well as overall phosphorylation (Figure 1B). Treatment of liver cancer cell lines, SAMe-D, HepG2 or Huh7 with SAMe inhibited LARP1 protein expression by 45-60% compared to control (Figure 1C). *LARP1* mRNA levels remained unchanged upon SAMe treatment (Figure 1C). However, SAMe did not alter LARP1 protein or mRNA levels in normal mouse hepatocytes (Figure 1C).

SAMe treatment inhibits global and LARP1-mediated translation induction in liver cancer cell lines

SAMe treatment lowered protein translation rate (OPP fluorescence) by 58% in SAMe-D cells and by 83% in Huh7 cells compared to control but had no influence in normal mouse hepatocytes (Figure 2A). SAMe treatment did not exert any toxicity under the experimental conditions. SAMe treatment inhibited endogenous and over-expressed LARP1 protein expression in Huh7 cells by 60-70% compared to empty vector (EV) control without a change in mRNA level (Figure 2B). LARP1 overexpression in Huh7 cells increased translation rate by 1.7-fold compared to EV+control (Figure 2C). SAMe treatment inhibited basal translation by 88% when compared to EV and LARP1-mediated translation by 75% when compared to LARP1 OV (Figure 2C).

LARP1 induces growth, migration, and invasion of liver cancer cell lines

LARP1 overexpression increased growth of Huh7 and Hep3B cells by 1.2-1.3-fold compared to EV whereas silencing *LARP1* had the opposite effect (Figure 3A). *LARP1* overexpression induced the migration of Huh7 and Hep3B cells by 1.3-fold compared to EV, whereas *LARP1* silencing inhibited migration by 30-40% compared to negative control siRNA (NC) (Figure 3B). The invasiveness of Huh7 and Hep3B cells was induced upon *LARP1* overexpression (2-2.5-fold vs. EV) and reduced by 45-65% upon *LARP1* silencing (Figure 3C).

TOP mRNA-encoded proteome induced in *Mat1a*-KO and in LARP1-overexpressing SAMe-D cells, is inhibited by SAMe administration

Phosphorylated LARP1 is known to induce translation of mRNAs containing TOP sequences[7]. Since we found LARP1 phosphorylation to be induced during SAMe deficiency and inhibited by SAMe treatment (Figure 1, Tables 1 and 2), we examined whether TOP mRNA-encoded protein expression was influenced under these conditions. Proteomics of *Mat1a*-KO livers showed a 1.4-1.5-fold induction of several TOP-proteins compared to WT that were strongly inhibited by SAMe administration (Figure 4A). *LARP1* overexpression in SAMe-D cells enhanced TOP-protein expression and SAMe treatment inhibited *LARP1*-mediated TOP induction (Figure 4B).

6

LARP1 expression is induced in human NAFLD and HCC

Immunohistochemical analysis and western blotting of human NAFLD tissues (simple steatosis, NASH, cirrhosis) revealed that LARP1 protein was induced by 4-15-fold in NAFLD compared to normal liver (Figure 5A). LARP1 protein was highly induced in human HCC (10-fold) compared to adjacent non-tumorous liver tissues without a change in mRNA level ((Figure 5B). This was associated with an induction of several TOP-proteins (RPL15, RPS3, RPL14, and EEF1A1) (Figure 5B).

Effects of site-specific phosphorylation of LARP1 on translation, growth, migration, and TOP protein expression in liver cancer cells

Out of several LARP1 phosphorylation sites that were responsive to SAMe treatment, we identified four sites (T449, S471, S697, and S250) whose phosphorylation was induced both in 4-month *Mat1a*-KO (pre-disease condition) and 10-month *Mat1a*-KO (NASH condition). All four sites were sensitive to SAMe treatment. These sites were tested for their functional effect on translation, growth, and migration capacity, and TOP-protein expression of liver cancer cell lines. Using site-directed mutagenesis to generate T449A, S471A, S697A, and S250A phospho-mutations, we showed that the T449A and S471A mutations strongly inhibited the ability of WT LARP1 to induce translation (Figure 6A). The S697A and S250A mutations did not significantly alter the translational activity of WT LARP1 (Figure 6A). The T449A and S471A mutations were further evaluated for their effect on cell growth, cell migration, and TOP-protein expression. Compared to WT LARP1, the T449A mutation was unable to induce growth in Huh7 and Hep3B cells (Figure 6B). The S471A mutation was still able to induce growth comparable to WT in Huh7 cells and was not as inductive as WT in Hep3B (Figure 6B). Consistent with its effect on growth, the T449A mutation significantly inhibited LARP1-mediated cell migration by 25-30% in both Huh7 and Hep3B cells (Figure 6C). Like the pattern observed for cell growth, the S471A mutation

inhibited LARP1-mediated migration of Hep3B but not of Huh7 cells (Figure 6C). We further evaluated the effect of T449A/S471A phospho-mutations and their corresponding phospho-mimetic mutations (T449E/S471E) on expression of oncogenic TOP ribosomal proteins, RPS3 and RPL15 in SAMe-D cells. RPL15 was not induced by LARP1 itself; however, the T449E phospho-mimetic mutant induced whereas a T449A phospho-mutation inhibited RPL15 expression (Figure 6D). The S471A mutation did not alter RPL15 expression (Figure 6D). Over-expression of LARP1 increased RPS3 protein level by 1.5-2-fold compared to EV. The S471A, but not the T449A mutation, inhibited LARP1-mediated RPS3 induction whereas S471E, the phospho-mimetic mutant, sustained RPS3 expression (Figure 6D). No changes in RP mRNA levels were observed with either WT or mutant over-expression (Figure 6D). Some TOP proteins induced in human HCC (RPL14 and EEF1A1, Figure 5B) were not significantly altered by T449 or S471 LARP1 phospho-site modifications (data not shown).

CDK2 and CK2 phosphorylate LARP1 protein

Since CDK2 and CK2 are predicted to phosphorylate LARP1 at sites that are SAMe sensitive (Table 1 and 2), we next investigated these kinases in direct phosphorylation of LARP1. Phosphorylation of recombinant LARP1 was significantly enhanced in the presence of active CDK2 or CK2 enzymes at 30°C compared to 0°C controls or in the absence of active kinases (Figure 7A). The in vitro kinase reactions of LARP1-CDK2 and LARP1-CK2 were further analyzed by mass spectrometry to identify CDK2 and CK2 phospho-sites. Out of five sites identified, four were confirmed to be CDK2 sites and one site was a CK2 site (Table 3). Silencing of CDK2 in Huh7 cells lowered phospho-immunoprecipitated LARP1 by 65% compared to NC with a 23% decrease in total LARP1. The phospho/total ratio was decreased by 60% compared to NC (Figure 7B). The phospho-proteome of *CDK2*-silenced cells showed an inhibition of several LARP1 phospho-sites compared to NC (Figure 7C). This was associated with a decrease in expression of several TOP-encoded proteins (Figure 7D). Even though CK2 phosphorylated recombinant

8

LARP1 (Figure 7A and Table 3), silencing CK2 did not alter the phosphorylation or content of

LARP1 in Huh7 cells (data not shown).

DISCUSSION

Downregulation of *MAT1A* in human NAFLD, HCC, and in mouse models causes depletion of liver SAMe reserves[1,3,4]. We have previously observed several kinases are sensitive to SAMe content, specifically they become activated when SAMe level falls and inhibited upon SAMe repletion[1]. This prompted us to investigate the liver phosphoproteome under SAMe deficiency to better understand the consequences of SAMe deficiency. We focused our investigation on LARP1 because the most striking pathway upregulated is protein translation and LARP1 hyperphosphorylation, both of which were inhibited by SAMe. We therefore focused on the phospho-sites of LARP1 that are SAMe sensitive.

LARP1 is the link between mTORC1 and protein translation, as phosphorylation of LARP1 by mTORC1 releases the inhibition that LARP1 exerts on protein translation. Subsequently phospho-LARP1 facilitates mTORC1-dependent translation initiation[7]. We have found LARP1 hyperphosphorylation and increased translational machinery components in the *Mat1a*-KO model. LARP1 modulation during SAMe deficiency has not been examined before but recent work provided a link between SAMe levels and mTORC1 signaling[19]. Using in vitro HEK293-overexpression systems, it was shown that SAMTOR is a novel regulator of mTORC1 signaling. SAMe directly interacts with SAMTOR at a dissociation constant of ~ 7µM. SAMe concentrations lower than 7µM facilitate SAMTOR binding to GATOR1 (GTPase activating protein for RagA/B, that translocates mTORC1 to the lysosomal surface when activated by amino acids). Binding of GATOR1 to SAMTOR inhibits mTORC1 signaling[19]. According to this scenario, low SAMe reserves may inhibit whereas high SAMe level may enhance mTORC1 signaling. However, from our data in the *Mat1a*-KO liver, it appears that mTORC1 activity (Ser-2448 phosphorylation) is higher during SAMe deficiency and is strongly inhibited by increasing SAMe levels in the liver. We speculate that the mechanism of SAMe-sensing described by Gu et al[19] may not be applicable

in the liver because the MATα1 enzyme provides a much higher steady state SAMe level of 50-100µM in hepatocytes[20]. This would cause constitutive mTORC1 activation in hepatocytes and this does not appear to be true under normal conditions. In fact, chronic mTORC1 activation results in HCC development due to ER stress and autophagy dysregulation[21]. We have discovered that LARP1 phosphorylation as well as protein content is induced during SAMe deficiency and not only does SAMe inhibit LARP1 phosphorylation and protein level, it also inhibits LARP1's translational activity. SAMe strongly suppressed LARP1 protein in multiple HCC cell lines but did not seem to alter its content in normal hepatocytes. One plausible explanation is that normal hepatocytes have high SAMe level[20] so that SAMe treatment may not be effective in regulating LARP1 as in the SAMe-deficient conditions of HCC cell lines.

Novel phospho-sites of LARP1 that are responsive to SAMe deficiency under pre-disease conditions (4-month *Mat1a*-KO) or in NASH (10-month KO) include T449, S471, S697, and S250. These sites were inhibited by SAMe treatment and most of them were predicted to be phosphorylated by CDK2 or CK2 kinases. We did not find any novel, mTOR-predicted phospho-site in this repertoire. A known mTOR-responsive site, S689[7] was found to show phosphorylation in the liver and in SAMe-D cells overexpressing LARP1 but did not respond to SAMe deficiency or replenishment. Interestingly, this site does not appear to be responsive to the changes in mTOR activity we found during SAMe deficiency. We found LARP1 content to be higher in human NASH, which has not been reported. We also found LARP1 to be enhanced in human HCC consistent with published findings[15].

We tested the hypothesis that alteration in LARP1 content and functionality during SAMe deficiency may regulate oncogenic activity. Increased LARP1 content by forced expression induced growth, migration, and invasiveness of liver cancer cell lines whereas silencing had the reverse effect. LARP1 phosphorylation by mTOR or AKT is known to increase its translational

11

activity on TOP mRNAs[7]. We therefore examined whether the novel LARP1 phospho-sites that we found during SAMe deficiency modulated its translational activity. Phospho-site mutations of LARP1-T449 and S471 dramatically reduced its ability to induce global translation whereas other sites such as S697 and S250 had no effect. We examined the effect of LARP1 phosphorylation on growth and migration in Huh7 cell line that grows aggressively with a doubling time of 23-27 hours and a slow growing Hep3B cell line with a doubling time of 41-53 hours[22]. The T449A mutation completely prevented LARP1's ability to induce growth and migration in both Huh7 and Hep3B cells. Despite its strong influence on global translation, the S471A mutation did not influence growth in Huh7 cells and only partially inhibited growth in Hep3B cells compared to WT LARP1. Consistent with its lack of effect on growth, the S471A mutant did not influence migratory potential of Huh7 cells but did inhibit LARP1's effect on Hep3B cell migration. The S471 phospho-site appeared to regulate growth/migration of slow growing Hep3B cells but was ineffective in modulating the phenotype of aggressively growing Huh7 cells. In contrast, the T449 phospho-site regulated HCC properties regardless of the cell's baseline growth characteristics.

In conjunction with LARP1 hyperphosphorylation, we found an overall surge in TOP mRNA-encoded protein expression under SAMe-deficient conditions (*Mat1a*-KO) that was sensitive to SAMe treatment. The data suggest a role of LARP1 hyperphosphorylation in inducing TOP-protein expression during SAMe deficiency and is further supported by the fact that forced expression of *LARP1* in SAMe-D cells enhanced TOP protein expression. Based on these data, we hypothesized that LARP1 phospho-sites control TOP translation activity causing increased expression of oncogenic RPs during SAMe deficiency. To evaluate the effect of LARP1 phosphorylation on TOP expression we chose two TOPs, RPS3 and RPL15 that we found to be highly induced in human HCC tissues[23]. RPS3 was also found by other researchers to be induced in HCC and associated with aggressive phenotype[24]. Recently, both RPL15 and RPS3 were found to be part of a 24-gene pro-oncogenic ribosomal gene signature that could be used for prognosis

of resectable HCC[14]. We found that forced expression of *LARP1* increased RPS3 protein level. The S471A but not the T449A mutant, inhibited LARP1-mediated RPS3 induction whereas S471E, the phospho-mimetic mutant, sustained RPS3 expression, suggesting that the LARP1-S471 site is important in regulating the translation of RPS3. RPL15 was not induced by LARP1 itself. One probable explanation for this could be that the over-expressed protein might not be completely phosphorylated in SAMe-D cells, allowing unphosphorylated LARP1 to interfere with RPL15 translation through 5'-UTR binding. This notion was supported by the finding that sustained phosphorylation caused by a T449E phospho-mimetic mutant induced RPL15 expression and a T449A phospho-mutant had the reverse effect. Despite its effect on the RPS3 protein, S471A mutations did not significantly influence RPL15 expression. Also, some other TOPs induced in HCC (RPL14 and EEF1A1) did not seem to be influenced by LARP1 phospho-sites. Hence only a subset of oncogenic TOPs appeared to be responsive to site-specific LARP1 phosphorylation.

By in vitro kinase/mass spectrometry-based assays, we confirmed that predicted kinases, CDK2 and CK2, phosphorylated LARP1. The T449 along with S697, T101, and S444 sites were confirmed as CDK2 sites. Only one site (S843) of LARP1 was phosphorylated by CK2 kinase. CDK2 emerged as a novel kinase phosphorylating LARP1 at multiple sites. In line with this result, CDK2 silencing in Huh7 cells reduced overall LARP1 phosphorylation and site-specific phosphorylation at several sites including T449 that is a functional CDK2 site. This was associated with a dramatic drop in several oncogenic TOPs including RPS3, RPL15 and RPL14 that we found to be induced in HCC. CK2 silencing did not significantly alter LARP1 phosphorylation. This could be explained by the smaller number of phosphorylation events mediated by this kinase.

In summary, our overall results show that modulation of the LARP1-T449 phospho-site and its associated kinase, CDK2, under SAMe deficient conditions regulates a subset of pro-oncogenic

13

RPs. The LARP1-T449 phosphorylation event is highly induced during SAMe deficiency, a condition known to be associated with NASH and HCC pathologies[2,3]. The T449 site positively regulates HCC parameters of growth, migration and invasiveness in liver cancer cells and may be a potential driver of NASH to HCC development during SAMe deficiency.

METHODS

Cell culture and treatments

Human HCC cell line, Huh7 was purchased from ThermoFisher Scientific (Rockford, IL). Human HCC cell lines, HepG2 and Hep3B were purchased from American Type Cell Collection (ATCC, Manassas, VA). The SAMe-D cell line, derived from HCC of a *Mat1a*-KO mouse, was previously described[25]. All cell lines were authenticated by the short tandem repeat profiling (STR) service (ATCC) and cultured according to our published methods[26]. Normal mouse hepatocytes were isolated from 3-4-month-old C57BL/6 mice according to an established protocol and plated on collagen-coated dishes[26]. S-adenosyl methionine (SAMe), in the stable form of disulfate p-toluene sulfonate dried powder was kindly provided by Gnosis SRL (Cairate, Italy). Cells cultured in 6-well plates (0.2 million per well) or 96-well plates (0.01 million cells per well) were treated with 0.5mM SAMe for 16 hours.

***Mat1a*-KO mouse model**

The *Mat1a*-KO mice and wild type (WT) littermate controls were described previously[27]. *Mat1a*-KOs at 4-months (pre-disease condition) and 10-months of age (NASH) were used in this study. For the 4-month old group, SAMe at 100mg/kg/day was administered by oral gavage for 7 days, which we showed normalized hepatic SAMe levels[28]. The 10-month old group consists of mice that had fatty liver on small animal ultrasound and elevated alanine aminotransferase and aspartate aminotransferase levels at 8-months of age and subsequently treated with vehicle or SAMe (30mg/kg/day by gavage 5 days per week) for 8 weeks[5]. All procedures for the care and use of mice were reviewed and approved by the Institutional Animal Care and Use Committee at Cedars-Sinai Medical Center (CSMC) and the CIC bioGUNE, Bilbao, Spain.

Human liver specimens

Normal human liver, NAFLD, HCC and adjacent non-tumorous tissues were procured from the Biobank and Translational Discovery Core at CSMC. The procedure for tissue collection and de-identification are approved by the Institutional Review Board at CSMC. All tissues were pathologically verified, snap frozen in liquid nitrogen and stored at −80°C. Some were also provided as unstained paraffin-embedded slides.

Plasmid Vectors and siRNA

Myc-DDK tagged *LARP1* vector and corresponding empty vector (EV) controls were purchased from Origene (Rockville, MD). Silencer select validated siRNAs for *LARP1*, cyclin-dependent kinase 2 *(CDK2)* and negative control (NC) were purchased from ThermoFisher Scientific.

Site-directed mutagenesis

Single amino acid changes that cause phospho-site mutations of serine/threonine to alanine (S/T to A) or phospho-mimetic mutations of serine/threonine to glutamic acid (S/T to E) were generated in the WT *LARP1* vector using the Quick Change II XL Site-Directed Mutagenesis Kit (Stratagene, La Jolla, CA) according to previously published protocols[29].

Transient transfection assays

Two micrograms of EV, *LARP1*, T449A/E-*LARP1*, S471A/E-*LARP1,* S697A-*LARP1,* S250A-*LARP1* vectors were transfected into 0.2 million cells in 6-well plates using jetPRIME® reagent (Polyplus-transfection, Radnor, PA) for 48 hours. For transfections in 10-cm dishes or 96-well plates, reagents and cells were scaled up or down according to manufacturer guidelines. NC, *LARP1*, *CDK2* or *CK2* siRNA was reverse transfected into 0.2 million cells at a concentration of 15nM using Lipofectamine® RNAiMAX (Invitrogen, Carlsbad, CA) for 48 hours according to the manufacturer's protocol. Transfection efficiencies were verified by real-time RT-PCR and western blotting.

Real-time RT-PCR

Total RNA was subjected to real-time RT-PCR using a published protocol[30]. Validated TaqMan gene expression probes for human or mouse *LARP1*, housekeeping genes, *HPRT1* (human), and *Gapdh* (mouse) were purchased from ThermoFisher Scientific. The thermal profile of real-time PCR consisted of the following: initial denaturation: 95°C for 3 minutes, 45 cycles; 95°C, 3 seconds; 60°C, 30 seconds. The CT (cycle threshold value of the target genes was normalized to that of control gene to obtain the ΔCT. The ΔCT was used to find the relative expression of target genes, according to the following formula: relative expression = 2−ΔΔCt, where ΔΔCT = ΔCT of target genes in experimental condition − ΔCT of target gene under control condition.

Western blotting and phostag™ assay

Total protein from cells or tissues was prepared using EDTA-free radioimmunoprecipitation assay buffer (RIPA) and subjected to western blotting[30]. Western blots probed with antibodies (Supplemental table 1) were quantified by densitometry using the ImageJ densitometry program (NIH). To detect phosphorylation of LARP1, phospho-protein was separated from unphosphorylated protein using phosTag™ molecule (Fujifilm Wako Chemicals, Richmond, VA) bound to zinc ions in a neutral gel system. Phostag binds to phosphorylated proteins and retards their mobility on a gel. Following an established protocol[29], proteins were run on 15uM-phostag gels. Separated proteins were immunoblotted with LARP1 antibody. Extracts treated with alkaline phosphatase (Sigma, St. Louis, MO) were used as a negative control to prove that the retarded bands were phosphorylated[29].

Co-Immunoprecipitation (Co-IP)

Co-IP of phospho-LARP1 from Huh7 cells with anti-phospho serine (PSer) antibodies was performed by incubating 500µg of cell extract with 2µg of antibody in RIPA buffer according to previously established protocols[30].

O-propargyl-puromycin (OPP) translation rate assay

Cells cultured in 96-well plates were treated with OPP-containing medium for 2 hours. The incorporation of OPP into actively translating polypeptides was detected by a fluorescent FAM-Azide based reaction following the instructions in the protein synthesis assay kit (Cayman Chemicals, Ann Arbor, MI). A fluorescence plate reader with a filter used to detect FITC (excitation/emission= 485/535nm) was used to measure OPP fluorescence.

Azido-homoalanine (AHA) translation assay

Cells transfected in 10-cm dishes for 48 hours were treated with the methionine analog, AHA (ThermoFisher Scientific), during the last 18 hours of transfection. A parallel set of cells cultured without AHA served as controls for AHA labeling. Cells were lysed in 1% SDS prepared in 50 mM Tris-HCl, pH 8.0, sonicated for 30 seconds and rotated at 4°C for 30 minutes. Proteins were estimated by A_{280} measurement. AHA-labeled and control extracts were subjected to a copper-catalyzed, biotin-alkyne labeling reaction to tag the AHA with biotin-alkyne via a click-chemistry reaction as reported[31]. Copper sulfate and other cofactors for the reaction (Tris(2-carboxyethyl) phosphine, Tris [(1-benzyl-1H-1,2, 3-triazol-4-yl) methyl]amine) were purchased from Sigma. Biotin-alkyne was purchased from ThermoFisher Scientific. The biotin-AHA labeled proteins were subjected to western blotting and probed with streptavidin-HRP antibody[31].

Cell Proliferation Assay

To assay for cell proliferation, cells plated in 96-well plates under different treatment conditions were incubated with bromodeoxyuridine (BrDU) according to our previously published method[32].

BrDU incorporation into DNA was measured using a plate reader at dual wavelengths of 450-540nm according to manufacturer's instructions (Millipore-Sigma, Burlington, MA).

Cell migration and invasion assays

Two-dimensional cell migration was measured using inserts for 6-well plates (Ibidi Inc., Fitchburg, WI) following manufacturer's instructions. Briefly, 0.4 million cells were seeded onto the radius of a 6-well plate using 2-D inserts and treated under different conditions described above. Photographic images of the cells were acquired immediately (0 hour) and after a 24 hour time period using an inverted microscope (EVOS XL core, Life technologies). The migration-occupied area at 24 hours was measured using the Image J software (NIH) and normalized to the area value at 0 hours for each condition. The invasion assay was performed using the BioCoat Matrigel Invasion Chamber (Corning, Tewksbury, MA). Briefly, 0.25 million cells were placed on the top insert. The bottom of the cell insert was covered with a filter containing multiple 8-μm pores and coated with a basement membrane matrix (Matrigel). Cells were seeded in the cell insert and placed in the wells. After 16 hours of attachment, the cells were treated under different conditions (described above) for an additional 24 hours. Invaded cells on the bottom of the insert membrane were detached and subsequently lysed and stained by CyQuant GR dye (ThermoFisher Scientific).

Immunohistochemistry

Paraffin-embedded sections of human liver tissue were subjected to antigen retrieval using a citric acid-based heating method (Abcam, Cambridge, MA). Slides were incubated with LARP1 antibody (1:50) or a normal rabbit IgG isotype control antibody (1:50) and developed using the HRP/DAB detection immunohistochemistry kit (Abcam). Stained slides were imaged at 20X magnification using an inverted microscope (EVOS XL core, Life technologies).

In vitro kinase assays

Full-length, human recombinant LARP1 protein (100ng, Novus Biologicals, Littleton, CO) was incubated with 225ng of active CDK2 or 8.3ng of active CK2 enzyme (Millipore-Sigma) in the presence of a magnesium/ATP cocktail (Millipore-Sigma) at 0°C or 30°C for 1 hour. The reaction mixture was immunoprecipitated with 0.5µg PSer antibody and immunoblotted with LARP1 antibody. LARP1 immunoprecipitated without incubation with CDK2 served as a -kinase control for the reaction. In vitro kinase reactions were subjected to mass spectrometry to identify LARP1 residues phosphorylated by CDK2 or CK2.

Data independent acquisition mass spectrometry analysis

Frozen mouse livers were homogenized under liquid nitrogen. Cells or homogenized livers were denatured in 8M urea buffer, sonicated (QSonica) at 4 °C for 10 minutes in 10 second pulses and centrifuged at 16,000 x g for 10 minutes at 4 °C. 100µg of the soluble extract from each sample was reduced with DTT (15mM) for 1 hour at 37 °C, alkylated with iodoacetamide (30mM) for 30min at room temperature in the dark, diluted to a final concentration of 2M Urea with 100mM Tris-HCl, pH 8.0 and digested for 16 hours on a shaker at 37 °C with a 1:40 ratio of Trypsin/Lys-C mix (Promega, Madison, WI). Each sample was de-salted using HLB plates (Oasis HLB 30µm, 5mg sorbent, Waters). Data independent acquisition mass spectrometry analysis was performed by preparing Lys PTM enriched peptide assay libraries as we recently reported[33]. For quantification of individual specimen DIA files, raw intensity data for peptide fragments was extracted from DIA files using the open source openSWATH workflow against the sample specific strong cation exchange (SCX) fractionated peptide assay as previously described[34]. The total ion current (TIC) associated with the MS2 signal across the chromatogram was calculated for normalization. This 'MS2 Signal' of each file was used to adjust the transition intensity of each peptide in a corresponding file. Normalized transition-level data were then processed using the mapDIA software[35] to perform pair-wise comparisons between groups.

Phosphorylation mass spectrometry analysis

Titanium Dioxide (TiO2) phospho enrichment was performed as previously described[36]. Briefly, 400ug of sample were digested as described above and individually de-salted on Oasis HLB cartridges (Water, 10mg) and eluted in 300µL of 80% acetonitrile (CAN), 5% trifluoroacetic acid (TFA), 1M glycolic acid. Each sample was then incubated in 50µL titanium dioxide (TiO2) slurry (30mg/mL, Glygen Corp, Columbia, MD) at room temperature on a shaker overnight. Then the TiO2 beads were washed twice with 200 µL of 80% ACN, 5% TFA, once with 200µL of 80% ACN, 0.1% TFA, and eluted in 180 µL of 30% ACN/ 1% NH4OH and neutralized with 200µL of 10% formic acid (FA). Samples were then desalted on Oasis HLB µ-elution plates (Waters) and eluted in 80% ACN, 0.1% FA, dried in speedvac, then resuspended in 0.1% FA for LC–MS/MS analysis.

Results from spectral searching through Trans-Proteomic Pipeline (TPP)[37] with a probability score of > 95% from the entire experimental dataset were imported into Skyline software for quantification of precursor extracted ion intensities (XICs)[38]. Precursor XICs from each experimental file were extracted against the Skyline library, and peptide XICs with isotope dot product scores>0.8 were filtered for final statistical analysis of proteomic differences. The Skyline documents containing precursor XICs from each experimental file are available at Panorama (Proteome exchange ID: PXD020015, https://panoramaweb.org/Larp1).

Statistical analysis

Data are represented as mean ± standard error (Mean±S.E.) from at least three experiments. Real-time PCR and densitometric analysis (as shown with each western blot) are expressed as percentage of controls. Statistical analysis was performed using analysis of variance followed by Fisher's test for multiple comparisons, and two-tailed Student's t-test for paired comparisons. For

changes in mRNA and protein levels, ratios of genes or proteins to housekeeping genes or proteins densitometric values were compared. Significance was defined as P<0.05.

REFERENCES

1. Lu SC & Mato J M. S-adenosylmethionine in liver health, injury, and cancer. *Physiol. Rev.* **92,** 1515-1542 (2012).

2. Murphy SK, Yang H, Moylan CA, Pang H, Dellinger A, Abdelmalek MF, Garrett ME, Ashley-Koch A, Suzuki A, Tillmann HL, Hauser MA, Diehl AM. Relationship between methylome and transcriptome in patients with nonalcoholic fatty liver disease. *Gastroenterology* **145,** 1076-1087 (2013).

3. Michelotti GA, Machado MV & Diehl AM. NAFLD, NASH and liver cancer. *Nat. Rev. Gastroenterol. Hepatol.* **10,** 656-665 (2013).

4. Noureddin M., Mato JM. & Lu SC. Nonalcoholic fatty liver disease: update on pathogenesis, diagnosis, treatment and the role of S-adenosylmethionine. *Exp. Biol. Med (Maywood)* **240,** 809-820 (2015).

5. Alonso C, Fernández-Ramos D, Varela-Rey M, Martínez-Arranz I, Navasa N, Van Liempd SM, Lavín Trueba JL, Mayo R, Ilisso CP, de Juan VG, Iruarrizaga-Lejarreta M, delaCruz-Villar L, Mincholé I, Robinson A, Crespo J, Martín-Duce A, Romero-Gómez M, Sann H, Platon J, Van Eyk J, Aspichueta P, Noureddin M, Falcón-Pérez JM, Anguita J, Aransay AM, Martínez-Chantar ML, Lu SC, Mato JM. Metabolic identification of subtypes of nonalcoholic steatohepatitis. *Gastroenterology* **152,** 1449-1461 (2017).

6. Fonseca BD, Zakaria C, Jia JJ, Graber TE, Svitkin Y, Tahmasebi S, Healy D, Hoang HD, Jensen JM, Diao IT, Lussier A, Dajadian C, Padmanabhan N, Wang W, Matta-Camacho E, Hearnden J, Smith EM, Tsukumo Y, Yanagiya A, Morita M, Petroulakis E, González JL, Hernández G, Alain T, Damgaard CK La-related Protein 1 (LARP1) Represses Terminal Oligopyrimidine (TOP) mRNA Translation Downstream of mTOR Complex 1 (mTORC1). *J. Biol. Chem.* **290,**15996-16020 (2015).

7. Hong S, Freeberg MA, Han T, Kamath A, Yao Y, Fukuda T, Suzuki T, Kim JK, Inoki K. LARP1 functions as a molecular switch for mTORC1-mediated translation of an essential class of mRNAs. *eLife* **6,** e25237 (2017).

8. Philippe L, Vasseur JJ, Debart F & Thoreen CC. La-related protein 1 (LARP1) repression of TOP mRNA translation is mediated through its cap-binding domain and controlled by an adjacent regulatory region. *Nucleic Acids Res.* **46,** 1457-1469 (2018).

9. Tcherkezian J, Cargnello M, Romeo Y, Huttlin EL, Lavoie G, Gygi SP, Roux PP. Proteomic analysis of cap-dependent translation identifies LARP1 as a key regulator of 5'TOP mRNA translation. *Genes Dev.* **28,** 357-371 (2014).

10. Aoki K, Adachi S, Homoto M, Kusano H, Koike K, Natsume T.. LARP1 specifically recognizes the 3' terminus of poly(A) mRNA. *FEBS Lett.* **587,** 2173-2178 (2013).

11. Zhou X, Liao WJ, Liao JM, Liao P. & Lu H. Ribosomal proteins: functions beyond the ribosome. *J. Mol. Cell Biol.* **7,** 92-104 (2015).

12. Xie X, Guo P, Yu H, Wang Y & Chen G. Ribosomal proteins: insight into molecular roles and functions in hepatocellular carcinoma. *Oncogene* **37,** 277-285 (2018).

13. Wang R, Wang X & Zhuang L. Gene expression profiling reveals key genes and pathways related to the development of non-alcoholic fatty liver disease. *Ann. Hepatol.* **15,** 190-199 (2016).

14. Grinchuk OV, Yenamandra SP, Iyer R, Singh M, Lee HK, Lim KH, Chow PK, Kuznetsov VA. Tumor-adjacent tissue co-expression profile analysis reveals pro-oncogenic ribosomal gene signature for prognosis of resectable hepatocellular carcinoma. *Mol. Oncol.* **12,** 89-113 (2018).

15. Roessler S, Jia HL, Budhu A, Forgues M, Ye QH, Lee JS, Thorgeirsson SS, Sun Z, Tang ZY, Qin LX, Wang XW. A unique metastasis gene signature enables prediction of tumor relapse in early-stage hepatocellular carcinoma patients. *Cancer Res.* **70,** 10202-10212 (2010).

16. Xie C, Huang L, Xie S, Xie D, Zhang G, Wang P, Peng L, Gao Z. LARP1 predict the prognosis for early-stage and AFP-normal hepatocellular carcinoma. *J. Transl. Med.* **11,** 272 (2013).

17. Shamsaei B, Chojnacki S, Pilarczyk M, Najafabadi M, Niu W, Chen C, Ross K, Matlock A, Muhlich J, Chutipongtanate S, Zheng J, Turner J, Vidović D, Jaffe J, MacCoss M, Wu C, Pillai A, Ma'ayan A, Schürer S, Kouril M, Medvedovic M, Meller J. piNET: a versatile web platform for downstream analysis and visualization of proteomics data. Nucleic Acids Res. 48: W85-W93 (2020).

18. Song C, Ye M, Liu Z, Cheng H, Jiang X, Han G, Songyang Z, Tan Y, Wang H, Ren J, Xue Y, Zou H. Systematic analysis of protein phosphorylation networks from phosphoproteomic data. Mol. Cell. Proteomics. 11:1070–1083 (2012).

19. Gu X, Orozco JM, Saxton RA, Condon KJ, Liu GY, Krawczyk PA, Scaria SM, Harper JW, Gygi SP, Sabatini DM. SAMTOR is an S-adenosylmethionine sensor for the mTORC1 pathway. *Science* **358,** 813-818 (2017).

20. Cai J, Mao Z, Hwang JJ & Lu SC. Differential expression of methionine adenosyltransferase genes influences the rate of growth of human hepatocellular carcinoma cells. *Cancer Res.* **58,** 1444-1450 (1998).

21. Menon S, Yecies JL, Zhang HH, Howell JJ, Nicholatos J, Harputlugil E, Bronson RT, Kwiatkowski DJ, Manning BD. Chronic activation of mTOR complex 1 is sufficient to cause hepatocellular carcinoma in mice. *Sci. Signal.* **5,** ra24 (2017).

22. Waldherr M, Mišík M, Ferk F, Tomc J, Žegura B, Filipič M, Mikulits W, Mai S, Haas O, Huber WW, Haslinger E, Knasmüller S. Use of HuH6 and other human-derived hepatoma lines for the detection of genotoxins: a new hope for laboratory animals? *Arch. Toxicol.* **92,** 921-934 (2018).

23. Yoshihama M, Uechi T, Asakawa S, Kawasaki K, Kato S, Higa S, Maeda N, Minoshima S, Tanaka T, Shimizu N, Kenmochi N. The human ribosomal protein genes: sequencing and comparative analysis of 73 genes. *Genome Res.* **12,** 379-390 (2002).

24. Zhao L, Cao J, Hu K, Wang P, Li G, He X, Tong T, Han L. RNA-binding protein RPS3 contributes to hepatocarcinogenesis by post-transcriptionally up-regulating SIRT1. *Nucleic Acids Res.* **47,** 2011-2028 (2019).

25. Vázquez-Chantada M, Ariz U, Varela-Rey M, Embade N, Martínez-Lopez N, Fernández-Ramos D, Gómez-Santos L, Lamas S, Lu SC, Martínez-Chantar ML, Mato JM. Evidence for LKB1/AMP-activated protein kinase/ endothelial nitric oxide synthase cascade regulated by hepatocyte growth factor, S-adenosylmethionine, and nitric oxide in hepatocyte proliferation. *Hepatology* **49,** 608-617 (2009).

26. Mavila N, Tang Y, Berlind J, Ramani K, Wang J, Mato JM, Lu SC. Prohibitin 1 Acts As a Negative Regulator of Wingless/Integrated-Beta-Catenin Signaling in Murine Liver and Human Liver Cancer Cells. *Hepatol. Commun.* **2,** 1583-1600 (2018).

27. Lu SC, Alvarez L, Huang ZZ, Chen L, An W, Corrales FJ, Avila MA, Kanel G, Mato JM. Methionine adenosyltransferase 1A knockout mice are predisposed to liver injury and exhibit increased expression of genes involved in proliferation. *Proc. Natl Acad. Sci. USA* **98,** 5560-5565 (2001).

28. Tomasi ML, Ramani K, Lopitz-Otsoa F, Rodríguez MS, Li TW, Ko K, Yang H, Bardag-Gorce F, Iglesias-Ara A, Feo F, Pascale MR, Mato JM, Lu SC. S-adenosylemthionine regulates dual-specificity MAPK phosphatase expression in mouse and human hepatocytes. *Hepatology* **51,** 2152-2161 (2010).

29. Ramani K, Donoyan S, Tomasi ML, Park S.. Role of methionine adenosyltransferase α2 and β phosphorylation and stabilization in human hepatic stellate cell trans-differentiation. *J. Cell. Physiol.* **230,** 1075-1085 (2015).

30. Ramani K, Tomasi ML, Berlind J, Mavila N & Sun Z. Role of A-Kinase Anchoring Protein Phosphorylation in Alcohol-Induced Liver Injury and Hepatic Stellate Cell Activation. *Am. J. Pathol.* **188,** 640-655 (2018).

31. Schiapparelli LM, McClatchy DB, Liu HH, Sharma P, Yates JR 3rd, Cline HT. Direct detection of biotinylated proteins by mass spectrometry. *J. Proteome Res.* **13,** 3966-3978 (2014).

32. Li J, Ramani K, Sun Z, Zee C, Grant EG, Yang H, Xia M, Oh P, Ko K, Mato JM, Lu SC. Forced expression of methionine adenosyltransferase 1A in human hepatoma cells suppresses in vivo tumorigenicity in mice. *Am. J. Pathol.* **176,** 2456–2466 (2010).

33. Robinson AE, Binek A, Venkatraman V, Searle BC, Holewinski RJ, Rosenberger G, Parker SJ, Basisty N, Xie X, Lund PJ, Saxena G, Mato JM, Garcia BA, Schilling B, Lu SC, Van Eyk JE. Lysine & Arginine Protein Post-translational Modifications by Enhanced DIA Libraries: Quantification in Murine Liver Disease. Preprint at https://doi.org/10.1101/2020.01.17.910943 (2020).

34. Parker SJ, Venkatraman V & Van Eyk JE. Effect of peptide assay library size and composition in targeted data-independent acquisition-MS analyses. *Proteomics* **16,** 2221-2237 (2016).

35. Teo G, Kim S, Tsou CC, Collins B, Gingras AC, Nesvizhskii AI, Choi H. mapDIA: Preprocessing and statistical analysis of quantitative proteomics data from data independent acquisition mass spectrometry. *J. Proteomics* **129,** 108-120 (2015).

36. Stachowski MJ, Holewinski RJ, Grote E, Venkatraman V, Van Eyk JE, Kirk JA. Phospho-Proteomic Analysis of Cardiac Dyssynchrony and Resynchronization Therapy. *Proteomics* **18,** e1800079 (2018).

37. Deutsch EW, Mendoza L, Shteynberg D, Farrah T, Lam H, Tasman N, Sun Z, Nilsson E, Pratt B, Prazen B, Eng JK, Martin DB, Nesvizhskii AI, Aebersold R. A guided tour of the Trans-Proteomic Pipeline. *Proteomics* **10**:1150–1159 (2010).

38. MacLean B, Tomazela DM, Shulman N, Chambers M, Finney GL, Frewen B, Kern R, Tabb DL, Liebler DC, MacCoss MJ. Skyline: an open source document editor for creating and analyzing targeted proteomics experiments. *Bioinformatics* **26**:966–968. (2010).

ACKNOWLEDGEMENTS

AUTHOR CONTRIBUTIONS

Komal Ramani identified and analyzed the LARP1/translational pathway from phospho-proteomics data, performed LARP1 phospho-analysis, translation and kinase assays (Figure 1, 6, 7, Tables 1, 2, 3); **Aaron Robinson** performed phospho-proteomics/proteomics assays, analyzed mass spectrometry data, performed analysis of LARP1 phosphorylation events, predicted kinases and TOP-encoded proteome (Tables 1, 2, 3, Figure 4); **Joshua Berlind** performed studies pertaining to LARP1 expression in mouse models/HCC cell lines, translation rate assays, mutant analysis, immunohistochemical and phospho-proteome analysis (Figure 1, Figure 2, Table 1, parts of figure 5 and 6); **Wei Fan** performed cell growth, migration and invasion assays (Figure 3 and 6); **Aushinie Abeynayake** performed siRNA/vector transfection, mutagenesis and western blotting (parts of Figure 5, 6, 7) and contributed to manuscript preparation; **Aleksandra Binek** performed phospho-proteomics and proteomics mass spectrometry; **Lucia Barbier-Torres** helped with western blotting; **Mazen Noureddin** provided human NAFLD liver samples; **Nickolas N. Nissen** provided human HCC samples; **José M. Mato** critically reviewed the phospho-proteomics/ proteomics data and contributed to manuscript review; **Jenny Van Eyk** provided the resources for all phospho-proteomics/proteomics assays and critically evaluated the data and manuscript; **Shelly C. Lu** obtained funding and provided overall supervision for the work, performed data analysis and manuscript preparation.

Table 1: Phospho-proteome analysis of LARP1 in 4-month and 10-month old WT and *Mat1a*-KO treated with SAMe or vehicle.

Conserved phospho-site (mouse/human)	Phospho-peptide sequence	Kinase prediction		4-month			10-month	
			WT	*Mat1a* KO vs. WT	*Mat1a* KO+SAMe vs. KO	WT	*Mat1a* KO vs. WT	*Mat1a* KO+SAMe vs. KO
T503/T449-LARP1	AV**T**PVPTKTEEVSNLK	CDK2	100	250	63	100	*190	**85
S525/S471-LARP1	GLSA**S**LPDLDSEQIEVK	Unknown	100	*234	**54	100	*113	**51
S751/S697-LARP1	SLPTTVPE**S**PNYR	CDK2	100	*199	**75	100	*182	**54
S302/S250-LARP1	VEPAWHDQDETSSVK**S**DGAGGAR	CK2	100	146	114	100	*283	**40
T151/T101-LARP1	VGDFGDAINWP**T**PGEIAHK	CDK2	ND	ND	ND	100	*900	**19
S897/S843-LARP1	FW**S**FFLR	CK2	ND	ND	ND	ND	ND	ND
S498/S444-LARP1	ETESAP**G**SPR	CDK2	100	85	124	100	ND	ND
#S743/S689-LARP1	**S**LPTTVPESPNYR	mTOR	100	70	80	100	175	74
#S824/S770-LARP1	TA**S**ISSSPSEGTPTVGSYGCTPQSLPK	AKT	ND	ND	ND	ND	ND	ND

Livers were processed for mass spectrometry analysis as described under Methods. The intensity of phospho-enriched peptides was normalized to that of total LARP1. Results represent Mean±SE from 5 experiments expressed as a percentage of WT. *p<0.05 vs. WT. **p<0.05 vs. KO. #=known phosphorylation events[7]. ND=not detectable.

Table 2: Phospho-proteome analysis of LARP1 in *LARP1*-overexpressing SAMe-D cells with or without SAMe treatment.

Conserved phospho-site (mouse/human)	Phospho-peptide sequence	Kinase prediction	*LARP1*-OE SAMe-D cells	*LARP1*-OE SAMe-D+SAMe
T503/T449-LARP1	AV**T**PVPTKTEEVSNLK	CDK2	100	*40
S525/S471-LARP1	GLSA**S**LPDLDSEQIEVK	Unknown	100	31
S751/S697-LARP1	SLPTTVPE**S**PNYR	CDK2	100	*62
S302/S250-LARP1	VEPAWHDQDETSSVK**S**DGAGGAR	CK2	100	112
T151/T101-LARP1	VGDFGDAINWP**T**PGEIAHK	CDK2	ND	ND
S897/S843-LARP1	FW**S**FFLR	CK2	100	*41
S498/S444-LARP1	ETESAP**G**SPR	CDK2	100	*77
#S743/S689-LARP1	**S**LPTTVPESPNYR	mTOR	100	114
#S824/S770-LARP1	TA**S**ISSSPSEGTPTVGSYGCTPQSLPK	AKT	ND	ND

SAMe-D cells were processed for mass spectrometry analysis as described under Methods. The intensity of phospho-enriched peptides was normalized to that of total LARP1. Results represent Mean±SE from 4 experiments expressed as percentage of *LARP1*-OE. *p<0.05 vs. *LARP1*-OE. #=known phosphorylation events[7]. ND=not detectable.

Table 3: Mass spectrometry evaluation of CDK2 or CK2 phosphorylation sites in recombinant LARP1 protein.

Conserved LARP1 phospho-site (mouse/human)	Phospho-peptide sequence	% phospho-residues LARP1+CDK2	% phospho-residues LARP1+CK2	% phospho-residues LARP1 alone	Kinase for site
T503/T449	AV**T**PVPTKTEEVSNLK	75.6	10.9	19.6	CDK2
S751/S697	SLPTTVPE**S**PNYR	70.3	25.9	30	CDK2
T151/T101	VGDFGDAINWP**T**PGEIAHK	47	0	0	CDK2
S897/S843	FW**S**FFLR	47	90	42	CK2
S498/S444	ETESAP**G**SPR	79	33	46	CDK2

Recombinant LARP1 protein was incubated with active CDK2 or CK2 in an in vitro kinase reaction as described under Methods. Kinase reactions were processed by mass spectrometry to evaluate the sites phosphorylated by CDK2 or CK2. Results represent the average percentage of phospho-residues versus total protein from 3 experiments.
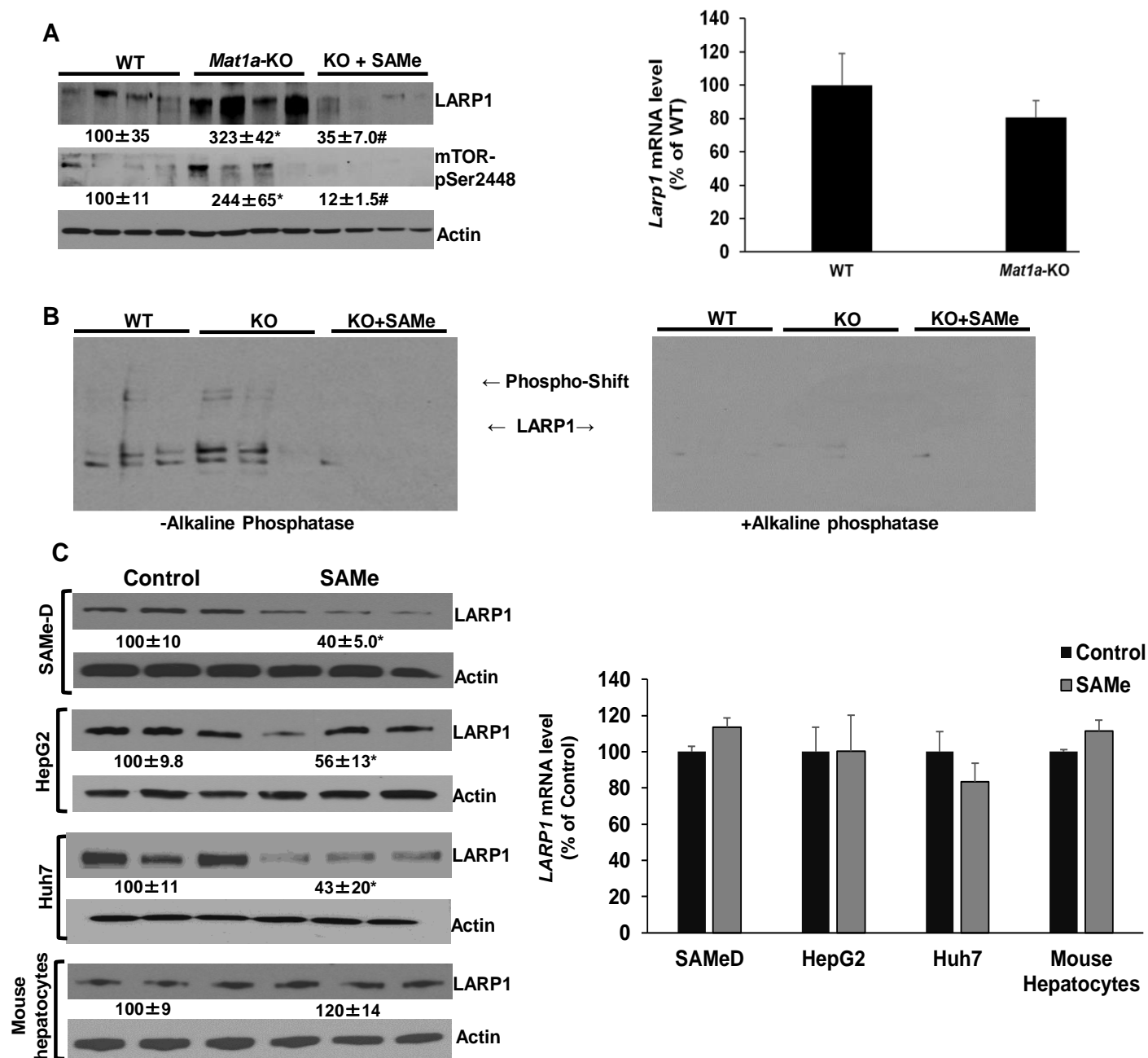
Figure 1. LARP1 protein expression is increased during SAMe deficiency and reduced by SAMe treatment. **A**. Left panel: LARP1 and phospho-mTOR (pSer 2448) protein levels in 10-month WT and *Mat1a*-KO livers±SAMe were measured by western blotting. Right panel: Total RNA was analyzed by real-time RT-PCR for *Larp1* or *Gapdh* (normalizing control). Mean±SE expressed as percentage of WT from 4 experiments. *p<0.05 vs. WT, #p<0.05 vs. WT and KO. **B**. LARP1 phosphorylation was assayed in WT or KO±SAMe protein using phostag™ western blotting as described under Methods. Extracts treated with alkaline phosphatase were used as a negative control to prove that the shifted bands were phosphorylated. **C**. SAMe-D, HepG2, Huh7, and primary mouse hepatocytes were treated with 0.5mM SAMe for 16 hours. Left panel: Total protein was analyzed by western blotting for LARP1 or actin (normalizing control). Right panel: *LARP1* mRNA was measured by real-time PCR. Mean±SE expressed as percentage of control from 3 experiments, *p<0.05 vs. control.
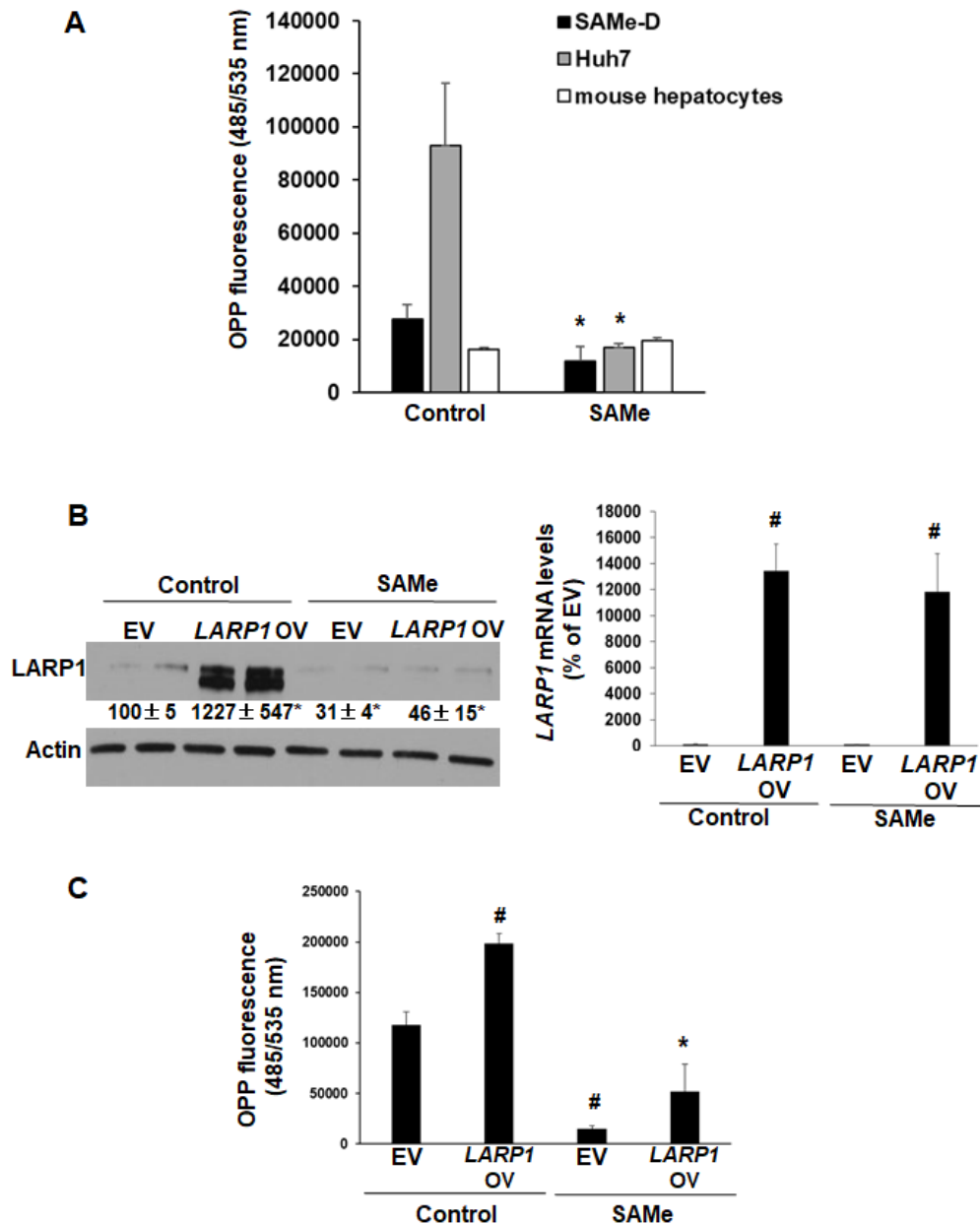
Figure 2. SAMe treatment inhibits global and LARP1-mediated translation induction in liver cancer cell lines. **A**. Translation rate in SAMe-D, Huh7, and primary mouse hepatocytes was measured by O-propargyl-puromycin (OPP) fluorescence as described under Methods. The incorporation of OPP into the C-terminus of translating polypeptides and its fluorescence detection using FAM-Azide as a readout of protein synthesis rate was measured using a plate reader. Mean±SE of OPP fluorescence from 4 experiments, *p<0.05 vs. control. **B**. Huh7 cells were transfected with *LARP1*-DDK vector in the absence or presence of SAMe treatment as described under Methods. **Left panel:** Western blot of *LARP1* overexpression (*LARP1* OV). Mean±SE as percentage of empty vector (EV) from 4 experiments, *p<0.05 vs. EV; **Right panel**: Real-time PCR of *LARP1* OV. Mean±SE as percentage of empty vector (EV) from 4 experiments, #p<0.01 vs. EV **C**. Translation rate in Huh7 cells by OPP florescence measurement as in 'A' above. Mean±SE of OPP fluorescence from 4 experiments. #p<0.01 vs. EV, *p<0.05 vs. EV or *LARP1* vector.
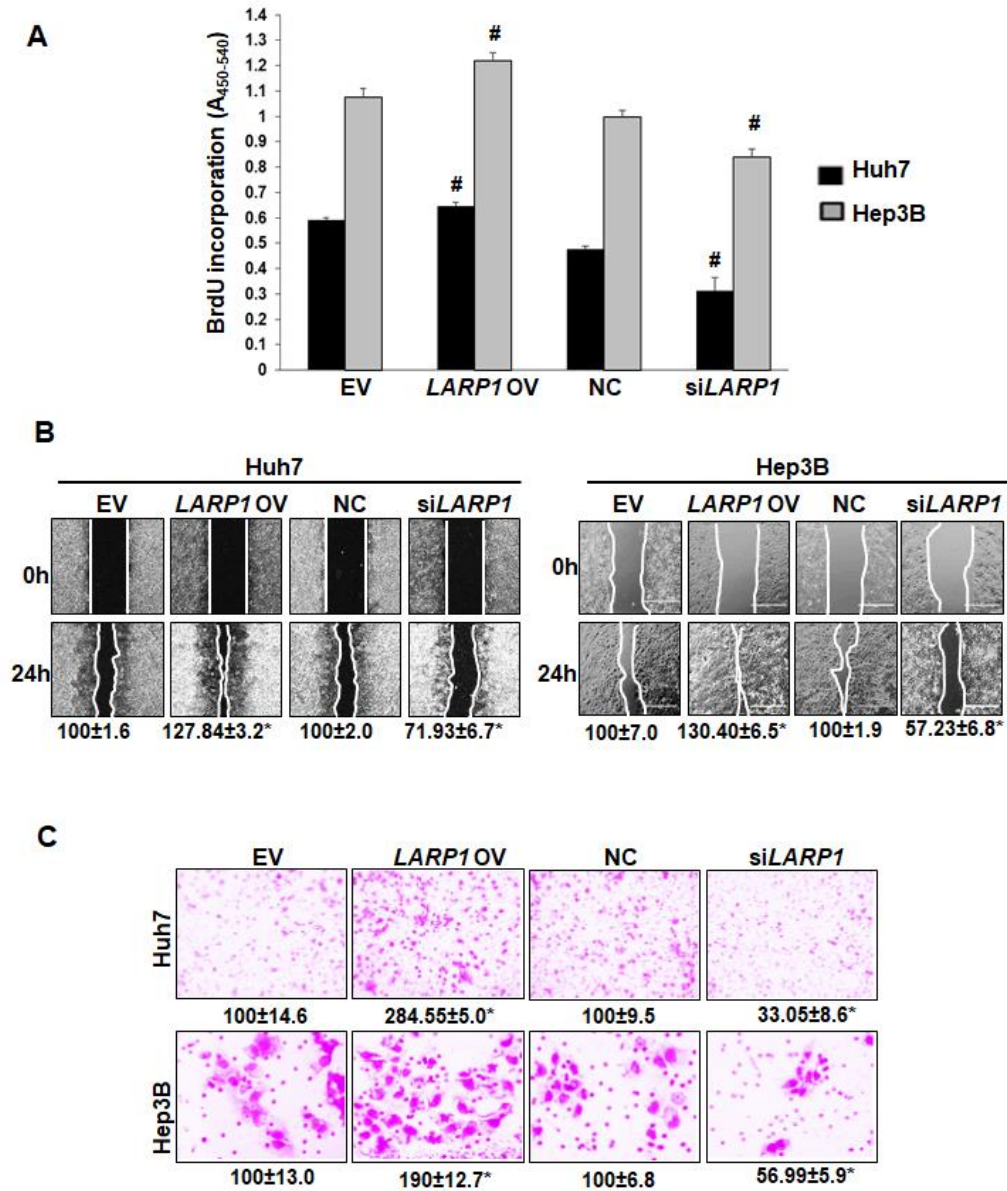
Figure 3. LARP1 induces growth, migration, and invasion of liver cancer cell lines. **A**. Huh7 or Hep3B cell lines were transfected with EV, *LARP1* vector (*LARP1* OV), negative control siRNA (NC) or *LARP1* siRNA (si*LARP1*) as described under Methods. Cell growth was assayed by the incorporation of bromodeoxyuridine (BrDU) into DNA as described under Methods. Mean±SE expressed as percentage of control from 3 experiments in duplicates. #p<0.01 vs. EV or NC. **B**. Huh7 and Hep3B cells were transfected as in 'A' and 2-D migration was assayed as described under Methods. Mean±SE expressed as percentage of control from 3 experiments in duplicates. *p<0.05 vs. EV or NC. **C**. Huh7 and Hep3B cells were transfected as in 'A' and invasion assays were performed as described under Methods. Mean±SE expressed as percentage of control from 3 experiments in duplicates. *p<0.05 vs. EV or NC.
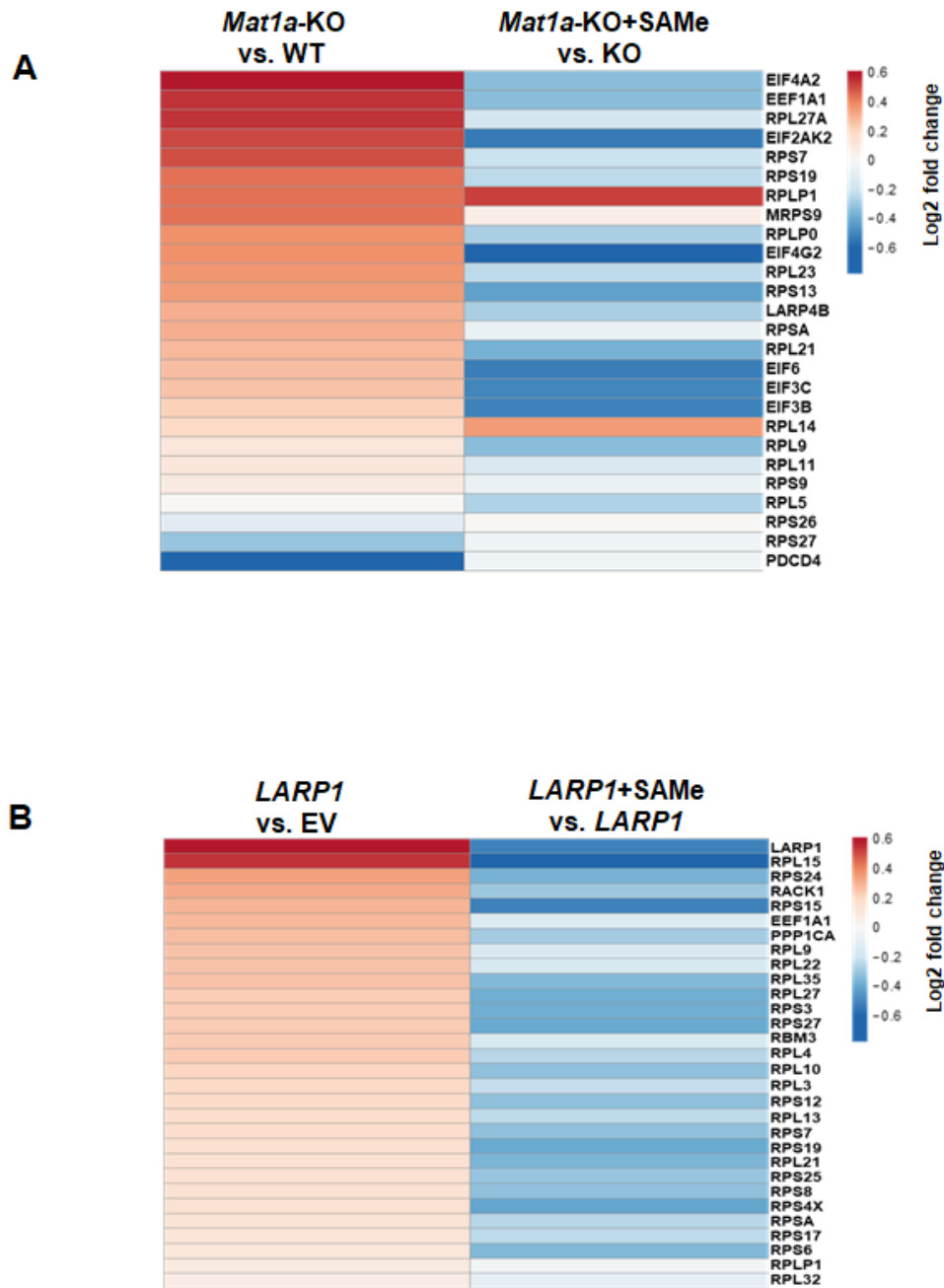
Figure 4. **TOP mRNA-encoded proteome induced in *Mat1a*-KO and *LARP1*-overexpressing SAMe-D cells, is inhibited by SAMe administration**. **A**. Total proteome of 10-month WT, *Mat1a*-KO or *Mat1a*-KO±SAMe was evaluated by mass spectrometry to identify TOP mRNA-encoded proteins. The data is represented as a heat map of fold changes of *Mat1a*-KO vs. WT and *Mat1a*-KO+SAMe vs. KO from 5 animals per group. P value less than 0.05 defines significance vs. respective controls. **B**. Total proteome of SAMe-D cells transfected with EV, *LARP1* vector or *LARP1* vector+SAMe treatment was evaluated by mass spectrometry to identify TOP-encoded proteins. The data is represented as a heat map of fold changes of *LARP1* vector vs. EV and *LARP1* vector+SAMe vs. LARP1 from 4 experiments. P value less than 0.05 defines significance vs. respective controls.
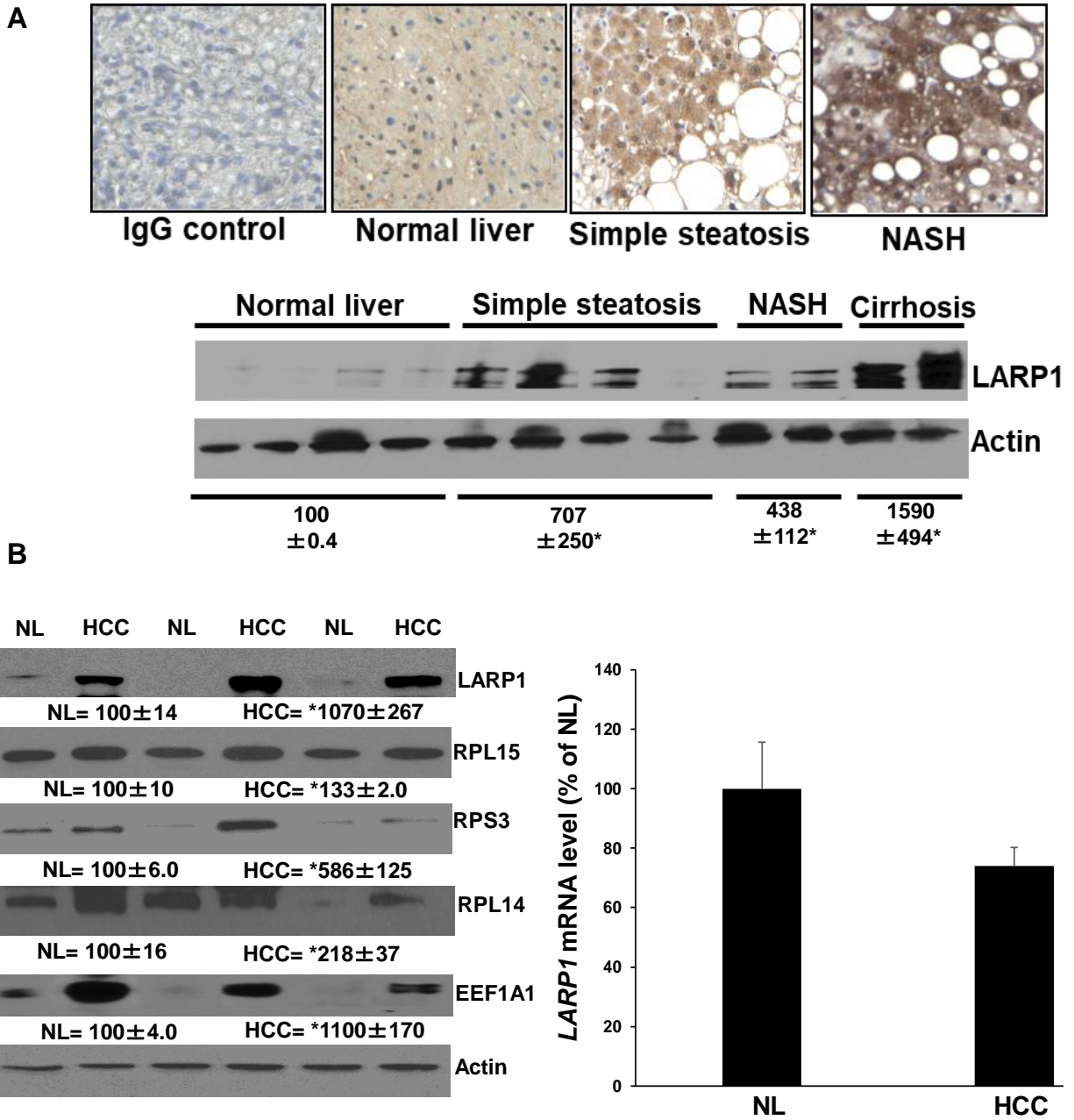
Figure 5. A. Top panel: **LARP1 is induced in human NAFLD**. Sections of NAFLD tissues (n=2 each) were stained for LARP1 protein using immunohistochemistry as described under Methods. **Bottom panel**: Western blotting of LARP1 was performed from liver extracts of different NAFLD stages and compared to normal liver. Mean±SE from 4 normal, 4 simple steatosis, 2 NASH and 2 cirrhosis livers are expressed as percentage of normal. *p<0.05 vs. normal. **B**. **LARP1 and TOP-encoded proteins are induced in human HCC**. Human HCC tissue and adjacent non-tumorous liver (NL) extracts were subjected to western blotting for LARP1, TOP-encoded proteins (RPL15, RPS3, RPL14, EEF1A1) and actin loading control (left panel) or real-time PCR for *LARP1* mRNA using *HPRT1* as a normalizing control (right panel). Mean±SE from 6 normal and 6 HCC tissues is expressed as a percentage of NL. *p<0.05 vs. NL. Three representative sets are shown in the figure.
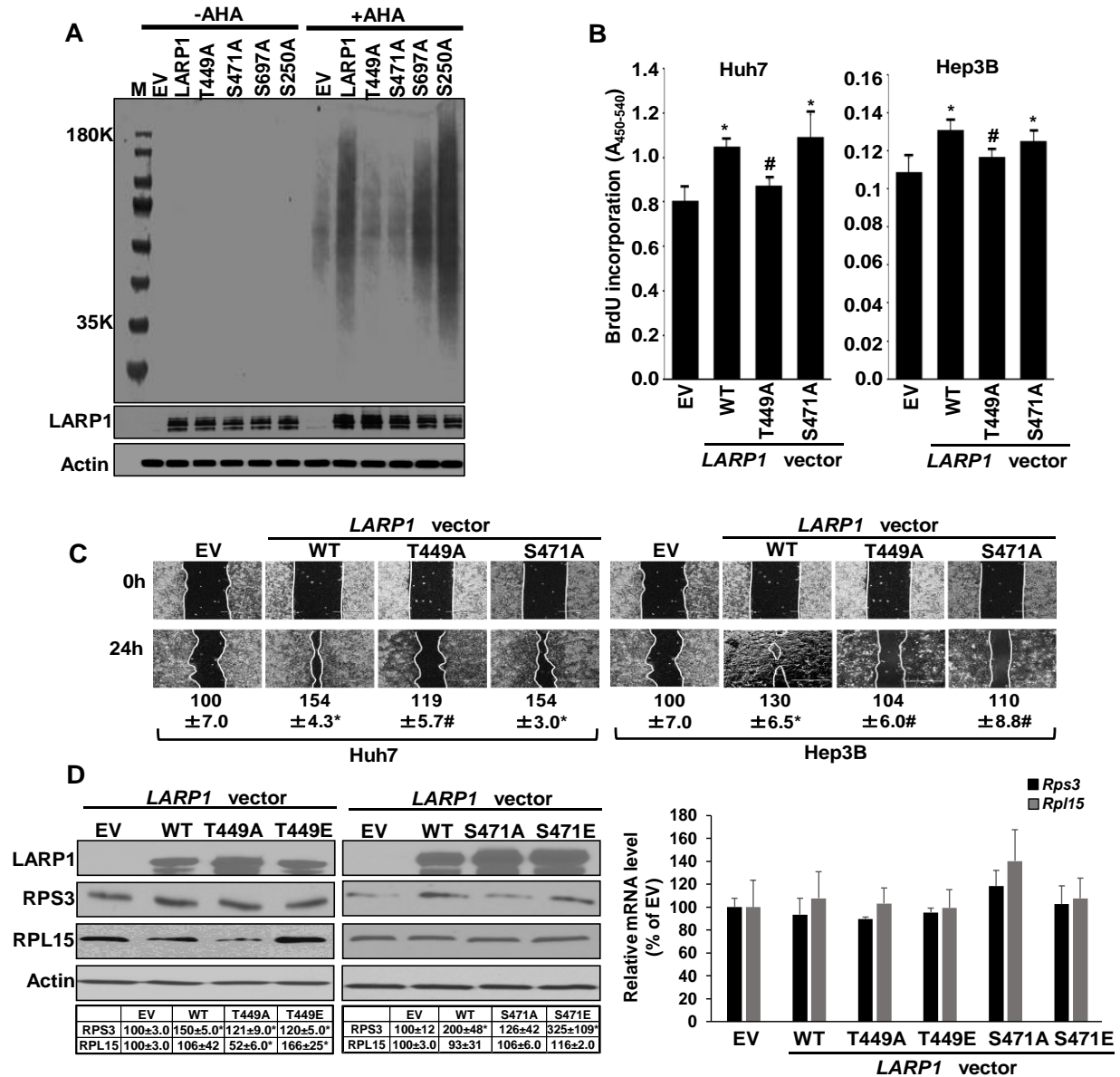
Figure 6. **Effects of site-specific phosphorylation of LARP1 on translation, growth, migration, and TOP protein expression in liver cancer cells**. **A**. Huh7 cells were transfected with empty vector (EV), WT *LARP1* vector or its phospho-site mutants, T449A, S471A, S697A, and S250A for 48 hours during which AHA was added to the culture medium. AHA-labeled proteins were detected as described under Methods. A representative western blot of AHA labeled proteins from 3 experiments is shown. **B**. Huh7 or Hep3B cells were transfected with EV, WT LARP1, T449A, and S471A mutants and BrDU incorporation was measured as described under Methods. Mean±SE expressed as percentage of EV from 4 experiments, *p<0.05 vs. EV, #p<0.05 vs. WT LARP1. **C**. Huh7 or Hep3B cells were transfected as in 'B' above and migration assays were performed as described under Methods. Mean±SE expressed as percentage of EV from 3 experiments in duplicates. *p<0.01 vs. EV, #p<0.01 vs. WT *LARP1*. **D**. SAMe-D cells were transfected with EV, *LARP1* or its phospho-site mutant vectors as described in Methods. Left panel: LARP1, TOP proteins (RPS3 and RPL15) and Actin were measured by western blotting. Right panel: *LARP1* or *Gapdh* (normalizing control) mRNA was measured by real-time PCR. Mean±SE expressed as percentage of EV from 3 experiments, *p<0.05 vs. EV.
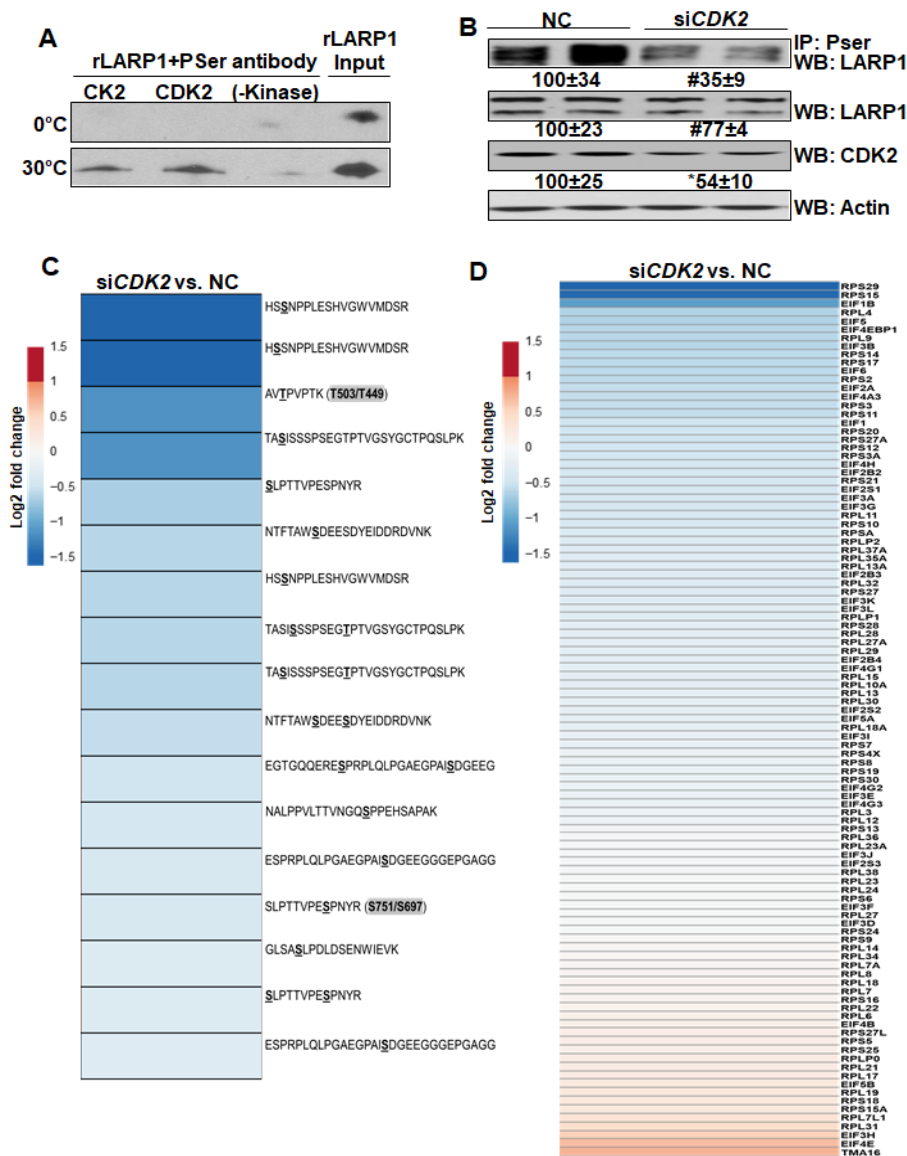
Figure 7. **CDK2 and CK2 phosphorylate LARP1 protein**. **A**. Recombinant, full-length LARP1 protein (rLARP1) was incubated with active CDK2 or CK2 enzymes in an in vitro kinase reaction at 0°C or 30°C (optimal kinase reaction temperature) as described under Methods. Samples without kinase were used as controls. The western blot represents phospho-serine (PSer) antibody immunoprecipitated LARP1 from three determinations. **B**. Huh7 cells were transfected with a negative control or *CDK2* siRNA for 48 hours as described under Methods. Phosphorylation of LARP1 (PSer immunoprecipitation), LARP1 and CDK2 expression was measured by western blotting. Mean±SE expressed as percentage of negative control from 3 experiments, *p<0.05, #p<0.01 vs. negative control. **C**. The phospho-proteome of negative control or *CDK2* siRNA-transfected Huh7 cells was evaluated by mass spectrometry for changes in LARP1 phospho-sites as described under Methods. The heat map represents fold changes versus negative control (NC) from 4 experimental groups. P value less than 0.05 defines significance vs. NC. **D**. The total proteome from negative control or *CDK2* siRNA-transfected cells was compared for TOP protein expression as described under Methods. The heat map is representative of fold changes vs. NC from 4 experiments. P value less than 0.05 defines significance vs. NC.

39

Supplemental Table 1: Antibodies used in this study.

Name	Citation (Pubmed ID)	Supplier	Cat no.	Clone no.
LARP1	29039571	Abcam	ab86359	Polyclonal IgG
Phospho-mTOR (pSer2448)	30794695	Cell Signaling Technology	2971	Polyclonal IgG
RPL15	29887867	Proteintech	16740-1-AP	Polyclonal IgG
RPS3	31620119	Proteintech	11990-1-AP	Polyclonal IgG
RPL14	24723395	Proteintech	14991-1-AP	Polyclonal IgG
EEF1A1	31561740	Proteintech	11402-1-AP	Polyclonal IgG
Anti-DDK (FLAG)	31831069	OriGene	TA50011-100	Monoclonal (Clone OTI4C5
Anti-Phosphoserine (PSer)	31938062	Abcam	Ab9332	Polyclonal IgG
CDK2	31985024	Proteintech	10122-1-AP	Polyclonal IgG
Anti-β-Actin−Peroxidase antibody (Control for *in vitro* experiments)	31772626	Millipore-Sigma	A3854	Monoclonal Clone (AC-15)
Normal rabbit IgG	21486814	Santa Cruz	Sc-207	Isotype control antibody